

Water-Soluble Cruciforms and Distyrylbenzenes: Synthesis, Characterization, and pH-Dependent Amine-Sensing Properties

Jan Freudenberg,[†] Jan Kumpf,[†] Vera Schäfer,[†] Eric Sauter,[†] Svenja J. Wörner,[†] Kerstin Brödner,[†] Andreas Dreuw,^{*,‡,§} and Uwe H. F. Bunz^{*,†,§}

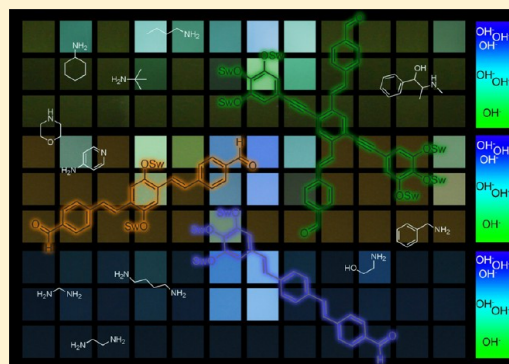
[†]Organisch-Chemisches Institut, Ruprecht-Karls Universität Heidelberg, Im Neuenheimer Feld 270, 69120 Heidelberg, Germany

[‡]Interdisziplinäres Zentrum für Wissenschaftliches Rechnen, Ruprecht-Karls Universität Heidelberg, Im Neuenheimer Feld 368, 69120 Heidelberg, Germany

[§]Centre of Advanced Materials (CAM), Ruprecht-Karls Universität Heidelberg, Im Neuenheimer Feld 225, Heidelberg, 69120 Germany

S Supporting Information

ABSTRACT: Three water-soluble fluorescent aldehyde-substituted distyrylbenzene derivatives were prepared using Heck or Horner methodologies. Water solubility was achieved through the addition of branched oligoethylene glycol side chains; these are attached via an ether bridge to the aromatic nucleus. The aldehydes are almost nonfluorescent in water, but addition of primary amines turns the fluorescence on; formation of imines results. Control of the basicity of the media allows further discrimination of the analytes employed. 1,3-Diaminopropane reacts with these aldehydes. Instead of an imine, a brightly fluorescent aminal forms. Amino acids are almost always nonreactive toward these aldehydes. Exceptions are lysine and cysteine, which form an imine and a thioaminal, respectively, discreating the aldehyde unit under fluorescence turn-on in water. The detection limit and time of completion of the sensing event were evaluated. Dialdehydes **3** and **16** were comparable on both counts. The cross-shaped **16** did react approximately twice as quickly with 1,3-diaminopropane.



INTRODUCTION

Here we give a full account of the amine-sensing prowess of water-soluble, aldehyde-appended distyrylbenzene fluorophores carrying branched oligoethyleneglycol side chains as solubilizing and fluorescence-enhancing substituents.¹ Photophysics, pH dependency, amine recognition, and modulation of the detection limit in water are discussed.

The detection and determination of amines is an attractive scientific task of added-on practical importance.² Amines are critical analytes in scenarios as different as industrial effluvia, bacterial infection, food spoiling, and cancer signatures; thus, amine detection might allow monitoring of disease states. A variety of chemosensory approaches toward the detection of amines exist, including but not restricted to water-soluble conjugated polymers, artificial receptor libraries, collections of hydrophobic porphyrin dyes,³ and also highly active trifluoromethyl-substituted ketones and some specific 1,3-diketones.^{4–10} These indicators work through a change of color upon reaction with an amine with a whole host of different mechanisms responsible for the recognition event. However, in most of the cases the colorimetric or fluorimetric amine recognition is performed in organic solvents. Notable exceptions are the conjugated polymers made by Lavigne et al. and the carbonyl compounds first prepared by Glass et al.

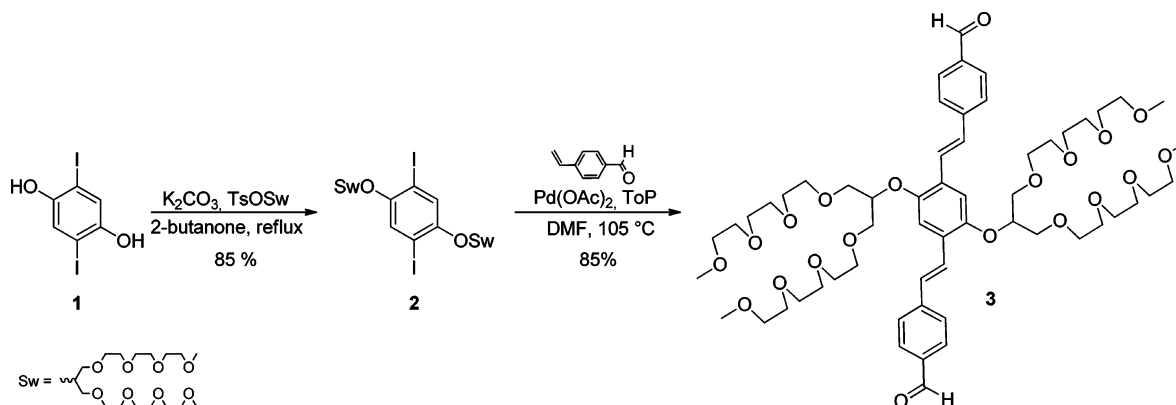
The synthesis of water-soluble distyrylbenzenes (DSB) carrying aldehyde groups, explored in our group, generates powerful fluorescence-based turn-on indicators for amines.¹¹

We have investigated amines as analytes for some time using cruciform (XF) fluorophores¹² and developed two different platforms. In tetrahydroxy-XFs,¹³ fluorescence change of the fluorophore results upon interaction with basic amines. Depending on the pK_a of the amine, hydrogen bonding or direct deprotonation of the phenolic XFs occurs and leads to a color change in emission, indicative of the chemical structure of the amine. This concept works well but needs high concentrations of the amine. To improve the sensitivity of the assay, we developed an amine dosimeter. Aldehyde-substituted distyrylbenzene-based and XF (2,5-bis(phenylethynyl)-1,4-distyrylbenzene)-based dialdehydes recognize primary, secondary, and 1,*n*-diamines. The starting XF or DSB dialdehydes were, if at all, almost nonfluorescent in water. The addition products with an amine, forming an imine, an aminal, or a hemiaminal, displayed enhanced fluorescence. The observed detection limit for the dialdehydes was considerably lower than that reported for the tetrahydroxy-XFs. The imines

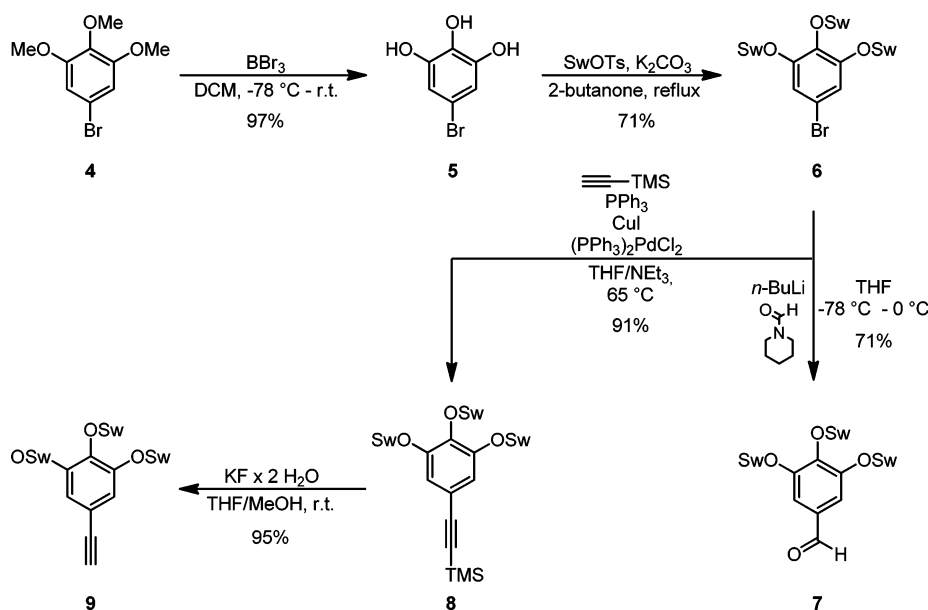
Received: March 20, 2013

Published: April 15, 2013

Scheme 1. Bulk Synthesis of 3



Scheme 2. Synthesis of Sw Building Blocks 7 and 9



can be made and easily isolated, being sensory materials in their own right.¹⁴ Here we have expanded our structural base and investigated water-soluble XFs and DSB-appended aldehydes as amine sensors.

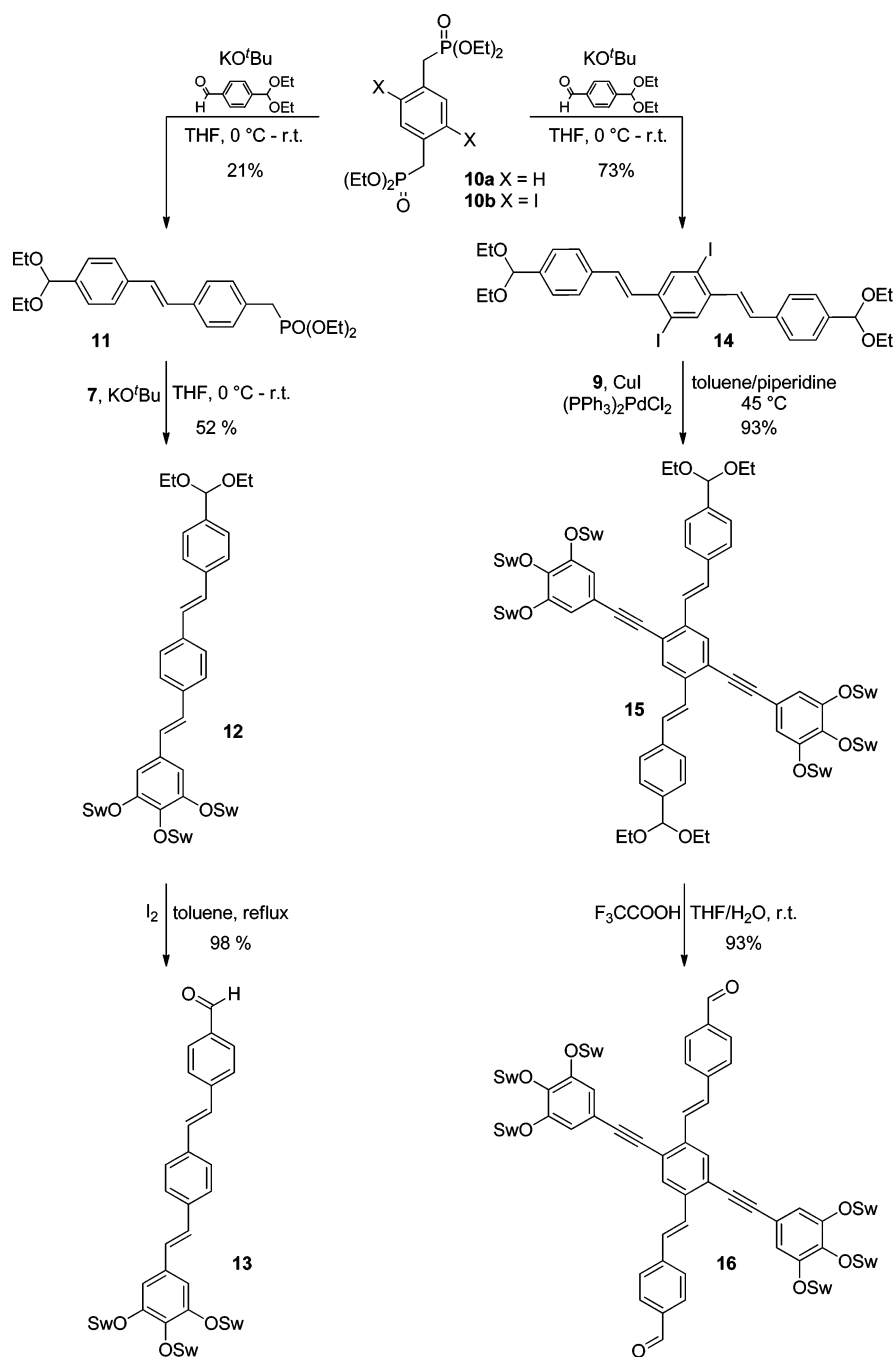
RESULTS AND DISCUSSION

Syntheses. Starting from **1**, alkylation with a branched oligoethyleneglycol-based tosylate (swallowtail tosylate, TsOSw) furnishes **2** in 85% yield (Scheme 1). A Heck reaction of the diiodide **2** with vinylbenzaldehyde employing tris(*o*-tolyl)phosphine (ToP) as ligand constructs the DSB derivative **3** in 85% yield. Overall (72%) this is an efficient synthesis of a sensory molecule. In the next step we planned the synthesis of the more complex target **16** and the monoaldehyde **13**. Both needed access to the intermediate **6**, which is obtained (Scheme 2) by demethylation of **4** and alkylation in satisfactory yields. The bromide **6** is now either subjected to halogen–metal exchange in THF, followed by treatment with *N*-formylpiperidine to give the aldehyde **7** (71%), or alkynylated by TMS-acetylene into **8** (91%) in a Sonogashira coupling. Deprotection of **8** by KF furnishes **9** as a colorless oil in almost quantitative yield.

In the second branch of the synthesis (Scheme 3) the bisphosphonate **10a** is treated with a monoprotected terephthalaldehyde to give compound **11** in fair yields. A second Horner reaction with **7** proceeds smoothly and furnishes the compound **12** in 52% yield as an inseparable mixture of *trans* and *cis* stereoisomers. Deprotection of the acetal and complete conversion to the all-*trans* aldehyde **13** is achieved upon addition of a catalytic amount of iodine. When bisphosphonate **10b**¹⁵ is treated with an excess of the monoprotected terephthalic aldehyde, **14** is isolated in 73% yield. Pd-catalyzed alkynylation of **14** smoothly affords **15**, almost quantitatively. Trifluoroacetic acid catalyzes hydrolysis of the acetals, and the target **16** forms in 93% yield on a 500 mg scale.

Spectroscopy. The spectroscopic properties of **13** and **3** in organic solvents and in water are shown in Figure 1. The absorption of the donor–acceptor fluorophore **13** is blue-shifted by 30 nm in comparison to that of **3** (Table 1). A similar effect is observed in emission. When water is used, where both fluorophores are soluble, the absorption spectra do not change but the emission spectra shift to the red, for **3** considerably more so than for **13** (Table 1). Also, the quantum yields drop dramatically in both cases, but more so for **3** (65% to 0.5%).

Scheme 3. Synthesis of Compounds 13 and 16



In Figure 2 we compare the optical properties of the bisacetal XF **15** with that of the dialdehyde **16**. **16**, with the larger π system, displays red-shifted absorption and emission. There is no difference in the absorption when going from dichloromethane into water, but the emission of **16** is red-shifted from 477 to 529 nm upon going into water. In **15** the red shift is only 10 nm when going from DCM into water. The fluorescence quantum yield of **16** in water is low (0.5%), while **15** emits with a robust 38% quantum yield in aqueous solution. However, the emissivity of **3** and **16** increases both when going into D₂O and when increasing the pH value to above pH 14. This increase suggests that **3** and **16** display pronounced excited state basicity in water and that hydrogen bonding is massively involved. To

gain more insight and understand this behavior, we performed quantum chemical calculations on the model compound **16m**.

To understand the strong decrease of fluorescence quantum yield of the aldehydes **3**, **13**, and **16** when going from a DCM to a water solution, the excited states and its properties **16m** were calculated (Figure 3), hydrogen bonded to two water molecules (time-dependent density functional theory (TDDFT),¹⁶ B3LYP exchange-correlation functional, standard cc-pVDZ basis set, Orca 2.9¹⁷). In addition to the two explicitly hydrogen bonded explicit water molecules, the conductor-like screening model (COSMO)¹⁸ includes the electrostatic effects of water solvation. Since we performed excited state geometry optimizations, hybrid functionals with large fractions of Hartree–Fock exchange were required to compensate for the

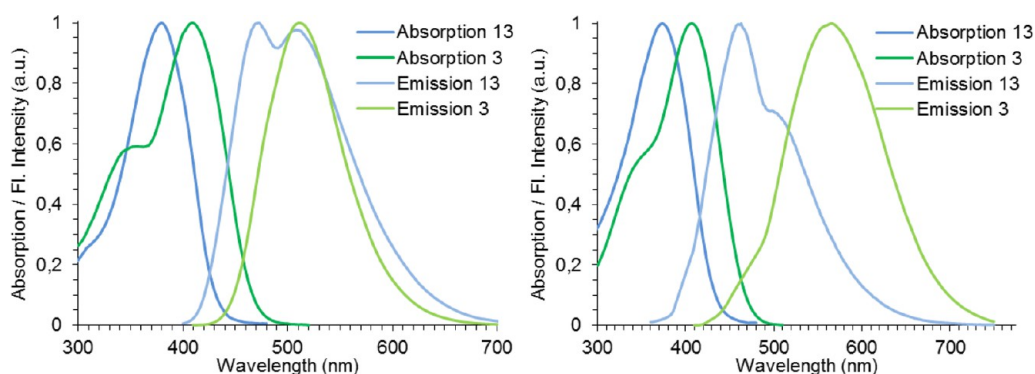


Figure 1. Absorption and emission spectra of 3 and 13 in dichloromethane (left) and in water (right).

Table 1. Photophysical Properties Recorded for 3, 13, 15, and 16 in DCM and in Water

compd	abs λ_{\max} (nm)	em λ_{\max} (nm)	Stokes shift (cm^{-1})	$\Phi_f \pm 10$ (%)	τ_f (ns)	ϵ ($\text{dm}^3/\text{mol cm}^{-1}$)
In DCM						
3	409	511	4880	65.3	1.2	29054
13	379	472, 508	5199	27.8	1.8	41544
15	340	447	7040	79.7	4.2	90503
16	351	477, 508	8805	22.5	3.4	70918
In Water						
3	407	565	6871	<0.5	n/a	39701
13	373	463, 510 sh	5211	2.4	1.7	37917
15	340	457	7530	37.5	5.3	67833
16	350	529	9668	0.5	0.3	64924

electron-transfer self-interaction error in TDDFT.¹⁹ At the ground state equilibrium geometry, the vertical excited states have been computed at the theoretical level of configuration interaction singles plus perturbative doubles (CIS(D)),²⁰ which describes charge-transfer excited states physically correctly. The results agree well with those calculated at the TDDFT/BHLYP level.

At the ground state equilibrium geometry (DFT/BHLYP/cc-pVDZ), the lowest excited state S_1 state corresponds to a one-photon allowed electronic transition from the HOMO to the LUMO. This is independent of the level of computation and the model of solvation; $n-\pi^*$ transitions do not play a role at all in **16m**. In water, S_1 is found at an excitation energy of 3.4 eV with a large oscillator strength of 2.7, corresponding to an absorption wavelength of 365 nm, which agrees well with the experimental absorption wavelength of **16**. Optimization of the

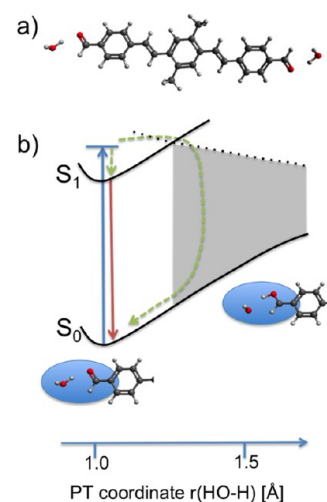


Figure 3. (a) Molecular model of the distyrylbenzene dialdehydes used for the computations. (b) Scheme of the excited state protonation pathway. Upon protonation a higher-lying excited state is strongly stabilized and, as soon as the potential energy surfaces cross, nonradiative decay is easily possible (gray shaded area).

geometry of **16m** in the first excited state does not lead to major geometric changes but does give a fluorescence wavelength of 420 nm. This is strongly blue shifted in comparison to the experimentally observed value in water; however, in the calculations solvent equilibration is missing, which is expected to stabilize the excited state and to lead to a substantial red shift of the fluorescence.

The increase of fluorescence intensity and lifetime of the dialdehydes in D_2O and strongly basic aqueous solution

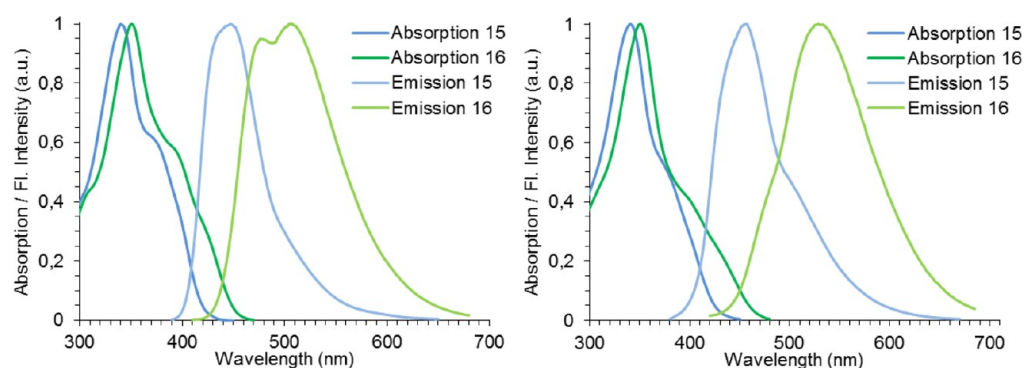


Figure 2. Absorption and emission spectra of 15 and 16 in dichloromethane (left) and in water (right).

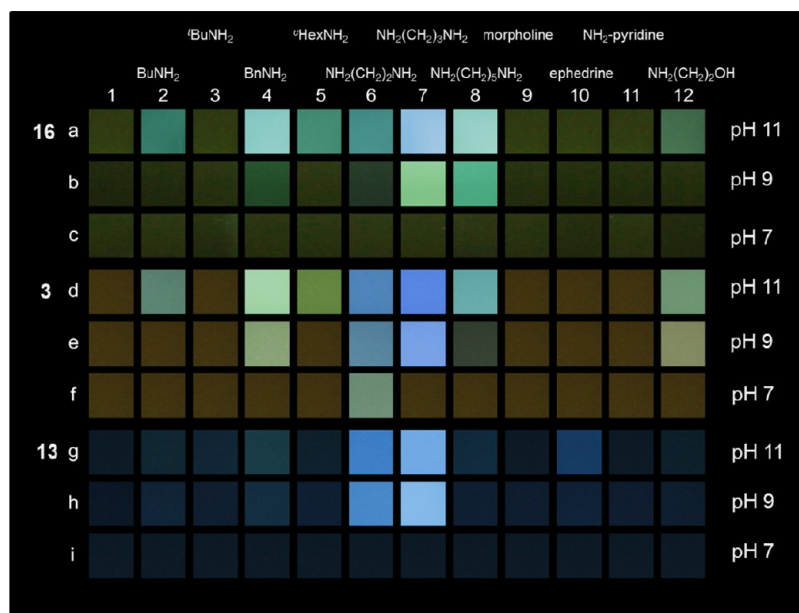


Figure 4. Photographs of buffered aqueous solutions ($c = 4.4 \mu\text{M}$) of **16** (a-c), **3** (d-f) and **13** (g-i) upon addition of amines 2–12 (left to right). Buffers: pH 11 ($\text{H}_3\text{BO}_3/\text{NaOH}/\text{KCl}$) (a, d, g), pH 9 ($\text{H}_3\text{BO}_3/\text{NaOH}/\text{KCl}$) (b, e, h), pH 7 ($\text{KH}_2\text{PO}_4/\text{Na}_2\text{HPO}_4$) (c, f, i). Columns: 1) Fluorophore reference, 2) butylamine (10.43), 3) *tert*-butylamine (10.45), 4) benzylamine (9.34), 5) cyclohexylamine (10.64), 6) ethylenediamine (6.90/9.95), 7) 1,3-diaminopropane (8.49/10.47), 8) cadaverine (9.58/10.85), 9) morpholine (8.36), 10) ephedrine (10.14), 11) 4-aminopyridine (9.12), 12) ethanolamine (9.50). The samples were excited using a hand-held UV-lamp at an emission wavelength of 365 nm. The numbers in parentheses give the pK_a of the ammonium salts.

suggests that excited-state protonation is involved in the fluorescence quenching mechanism. Therefore, the potential energy surfaces of the ground and lowest excited states have been computed along the protonation coordinate (Figure 3). While proton transfer in the ground state is not possible, as soon as the HO–H bond length of a hydrogen-bonded water molecule is stretched to 1.3 Å, a higher lying excited state crosses in that strongly stabilizes the proton transfer. This excited state corresponds to the transition of an electron from the HOMO-1 to the LUMO, which corresponds to an electron transfer from the hydroxide anion to the protonated aldehyde cation. In this state, the molecules can decay nonradiatively into the ground state via a conical intersection, nicely explaining the observed experimental fluorescence quenching of the dialdehydes; therefore, in water, the distyrylbenzene aldehydes serve as excited state bases which lead after intermolecular electron transfer and subsequent radiationless decay to back-transfer of the hydrogen atom to the OH radical.

Amine Sensing. Figure 4 shows a photograph of the interaction of aqueous solutions of the fluorophores **16**, **3**, and **13** with 11 different amines. The first column shows the fluorophores without any added amine. Columns 2–12 represent the colors that result after addition of an excess of the amines at pH 11, 9, and 7, respectively. From this photograph we glean that (a) morpholine, ephedrine, and 4-aminopyridine do not react at all (or only very weakly here with **13**), (b) propylenediamine and ethylenediamine promote turn-on of the fluorescence, and (c) primary amines with the exception of *tert*-butylamine also react with the fluorophores under turn-on of fluorescence.

The reactivity of the carbonyl compounds with amines is pH dependent. Control of the basicity of the aqueous solution results in additional selectivity with respect to the analytes. Under acidic or neutral conditions no reaction takes place, with the exception of **3** in the presence of ethylenediamine; some

turn-on occurs with a blue shift of the emission. The compound **13** is least reactive, i.e. most selective for ethylenediamine and propylenediamine; there are virtually no differences (except for the reaction with ephedrine) at pH 9 or 11. By visual inspection of the panel, one can easily distinguish all of the amines from each other (with the exception of the nonresponding ones).

To cross-validate our photographic experiments, we investigated solutions of the fluorophores **3**, **13**, and **16** in the presence of amines using absorption and emission spectroscopy (Figure 5). The top two rows show the reaction of **16** with the amines at pH 11 and 9. The most distinct change happens if **16** reacts with 1,3-diaminopropane. A strong and blue-shifted feature results through the formation of a cyclic aminal. The other amines also form an adduct, but the emission feature is between that of the proposed aminal and that of the dialdehyde. For the emission feature at 470 nm we suggest an imine to be responsible. We have investigated this issue for **3** in our preliminary communication and have now looked at **16** for further proof. Figure 6 shows ^1H NMR spectra of the adducts of **16** with 1,3-diaminopropane and with ethanolamine in D_2O .

16 features a signal diagnostic for the aldehyde proton at 10 ppm. Upon addition of 1,3-diaminopropane this signal disappears. A weak band at 8.3 ppm and a much more intense band at 4.5 ppm appear. The downfield-shifted signal belongs to the imine (*vide infra*), while the upfield signal is assigned to the formed aminal: it converts the aldehydes and pinches off the conjugation. A strongly blue-shifted emission results. The simple primary amines cannot react like this, but they form imines, also fluorescent and blue-shifted in comparison with the emission of **16**. Ethanolamine plus **16** efficiently form an imine, the distinct imine proton being visible at 8.3 ppm (Figure 6).

Having established a reasonable connection between structure and emission spectra at pH 11, fluorescence of **16** in the presence of 1,3-diaminopropane at pH 9 shows different characteristics. Here an aminal does not play a role at all, but an

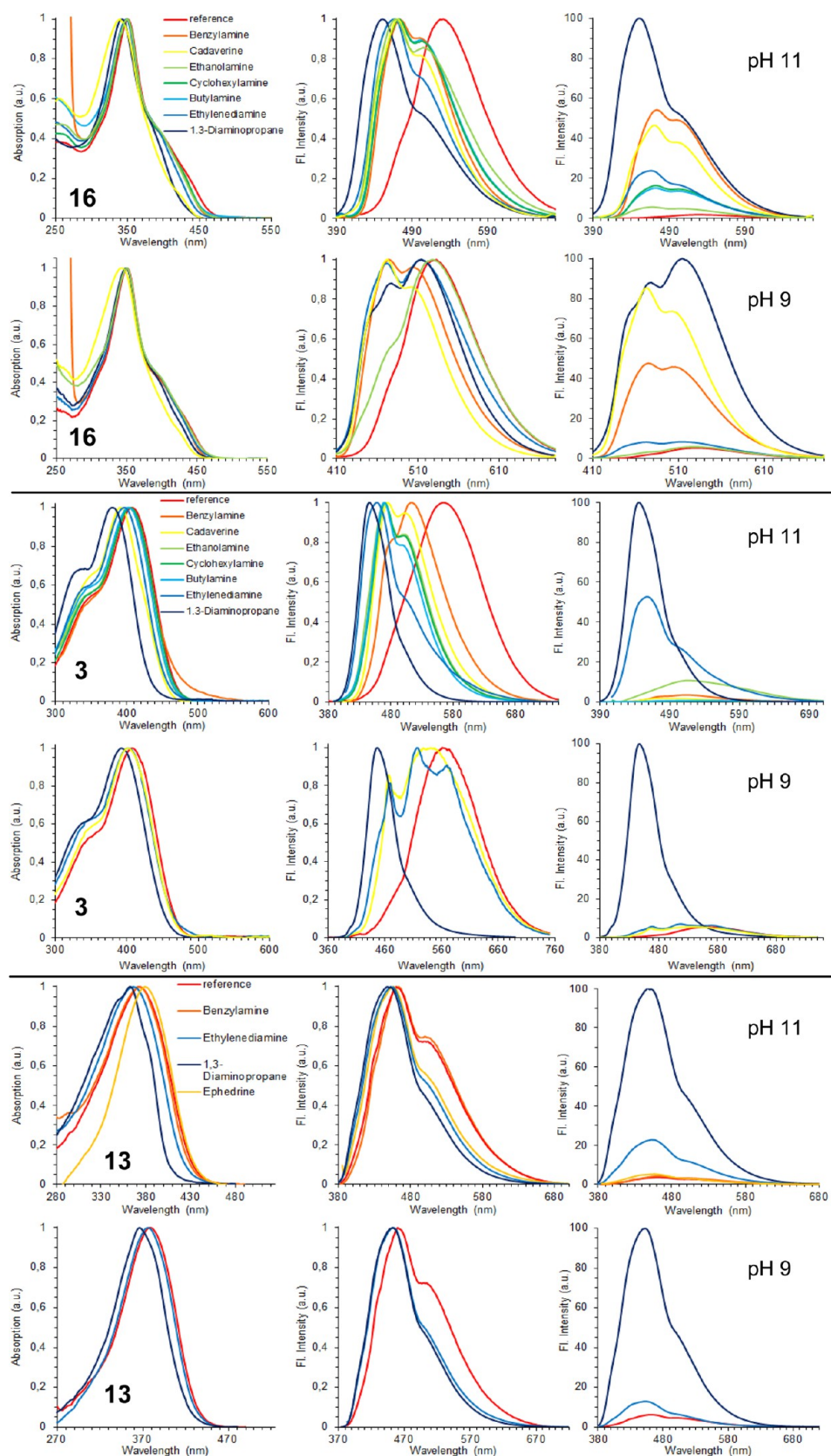


Figure 5. Absorption spectra (left), normalized emission spectra (middle), and non-normalized emission spectra (right) of buffered aqueous solutions (top, pH 11; bottom, pH 9) of 16, 3, and 13 upon addition of different amines.

imine is formed. This behavior can be accounted for by the difference in the acidities of the respective ammonium protons (vide supra). We ascribe the differing emission profiles and

intensities shown in Figure 5 to a changing mix of the monoimine, the bisimine, and the dialdehyde 16. Qualitatively similar observations are made for 3 and 13.

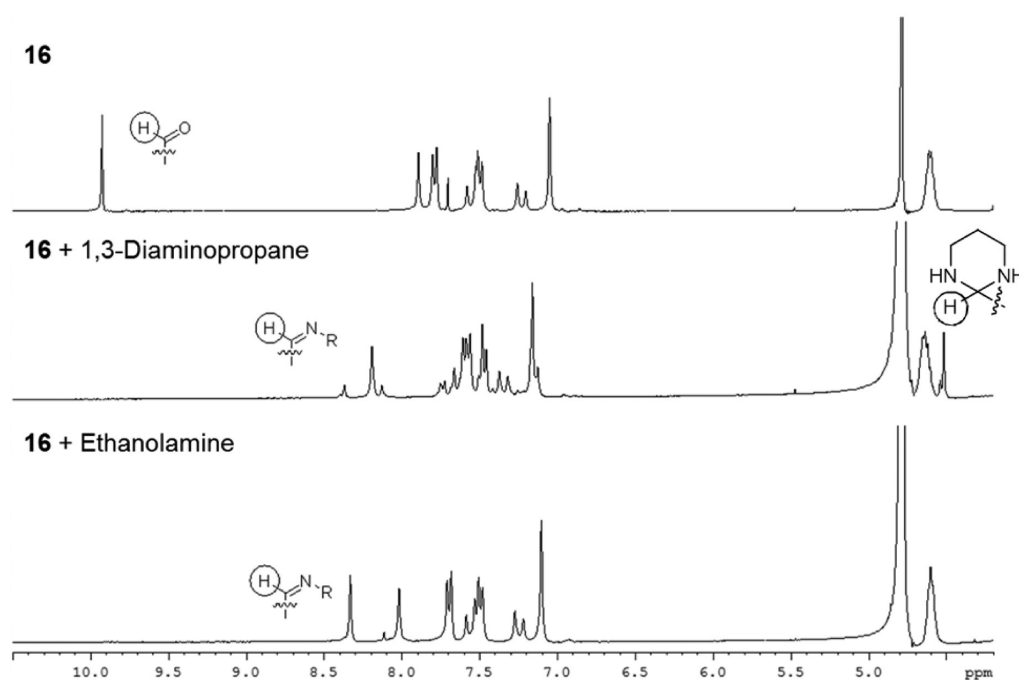


Figure 6. ^1H NMR spectra of **16** (15 mg in 0.5 mL of D_2O) in the presence of 1,3-diaminopropane (20 μL) and ethanolamine (20 μL). The top trace displays the spectrum of dialdehyde **16**.

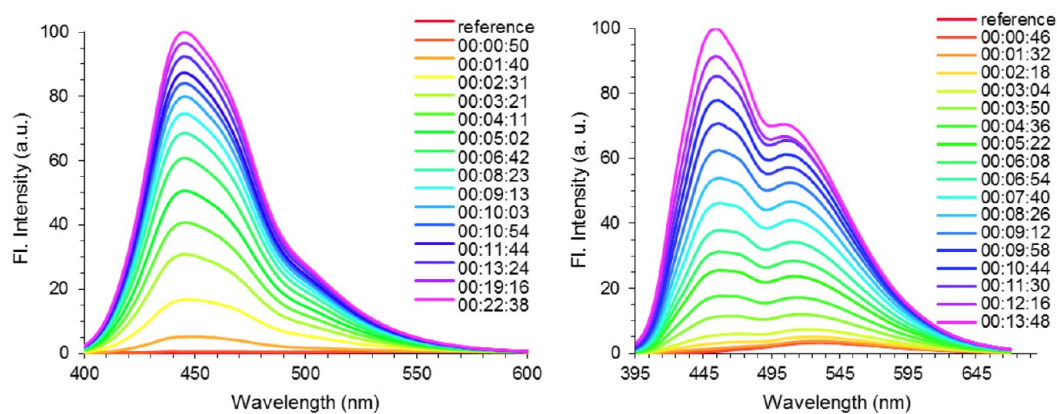


Figure 7. Time-dependent evolution of the emission wavelength and emission intensity for the reactions of **3** (left) and **16** (right) in an aqueous buffered solution (pH 11, $c = 0.9 \mu\text{M}$) with 1,3-diaminopropane (120 ppm (vol)).

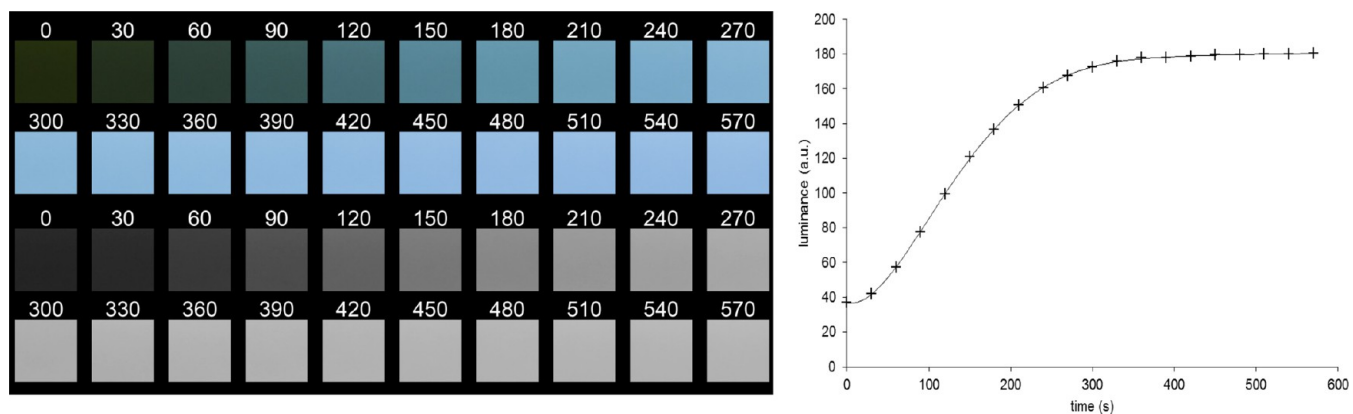


Figure 8. Time-dependent photographs of the fluorescence response of an aqueous solution ($c = 4.4 \mu\text{M}$, pH 11) of **16** after addition of 5 μL of 1,3-diaminopropane (left, time specification in s) and a luminance vs time plot (right).

How fast are the reactions of **3** and **16** with amines? Figures 7 and 8 show that both **3** and **16** react relatively quickly with 1,3-diaminopropane. Under the concentration regime chosen, the reaction is complete after around 0.5 h for **3** and after 0.25 h for **16**. The higher reactivity of **16**, surprising at first, stems from the somewhat electron-accepting arylethynyl substituents that make the aldehydes more electron accepting and therefore more reactive. If one uses higher concentrations of fluorophore and 1,3-diaminopropane, one can follow the reaction by photography (Figure 8). Under the chosen conditions, the reaction is finished after around 5 min. The data are just extracted from the brightness values of the photograph.

What is the detection limit for amines when using fluorophores such as **3** and **16** combined with 1,3-diaminopropane as the most reactive analyte? For both **3** and **16** (Figure 9) visible changes in fluorescence emission start at around 6 ppm of added amine and are distinct around 55 ppm of amine. Dialdehydes **3** and **16** both show roughly the same sensitivity toward amines.

The dialdehydes **3** and **16** detect amines in aqueous solution. It is of interest if amine-containing biomolecules would react with either **3** or **16** under fluorescence turn-on. Consequently, we treated solutions of **3** and **16** with the 20 natural amino acids at a concentration range of 4–8 mmol L⁻¹. Most of the amino acids do not react at all with the dialdehydes, as amino acids are reluctant to form imines.²¹ However, lysine forms imines with both **3** and **16**, while cysteine reacts after 1 h exclusively with **3**, probably forming a cyclic thioaminal in water, displaying bright blue fluorescence at pH 11 (Figure 10). However, the aldehydes are totally insensitive toward glutathione and mercaptoethanol, but they do react under turn-on with thioglycolic acetate at pH 11.

These compounds should form the basis of a highly applicable amine sensing platform. To achieve this and to increase the practicability of these sensory materials, we plan their integration into nonconjugated polymers. Thin films of these materials could be used as sensory materials for both amine vapors as well as for amine solutions. The immobilization would increase the concentration of the profluorophore and therefore increase the rate of reaction and the response time. Such materials would show broad applicability and use for sensitive amine detection.

CONCLUSION

We have prepared and investigated the three different DSB- and XF-based water-soluble aldehydes **3**, **13**, and **16** as amine and amino acid reactive sensory fluorophores. Fluorescence turn-on is observed upon reaction with primary amines and particularly diamines at high pH values. At pH 7 or below the aldehydes are unreactive toward the formed ammonium salts. Amino acids are generally nonreactive toward the aldehydes, with the exception of lysine (to both **3** and **16**) and cysteine (to **3**); an imine forms in the former case and a thioaminal in the latter. Overall, these aldehydes are attractive and powerful turn-on fluorophores for amines and specific amino acids. They work only at enhanced pH, and in neutral solution they are unreactive. Aldehydes are therefore a valuable addition to the growing quiver of amine-sensing materials working in aqueous solution. The surprisingly low fluorescence quantum yields of these dialdehydes in water could be explained by their excited state basicity, which leads to their surprising excited state.

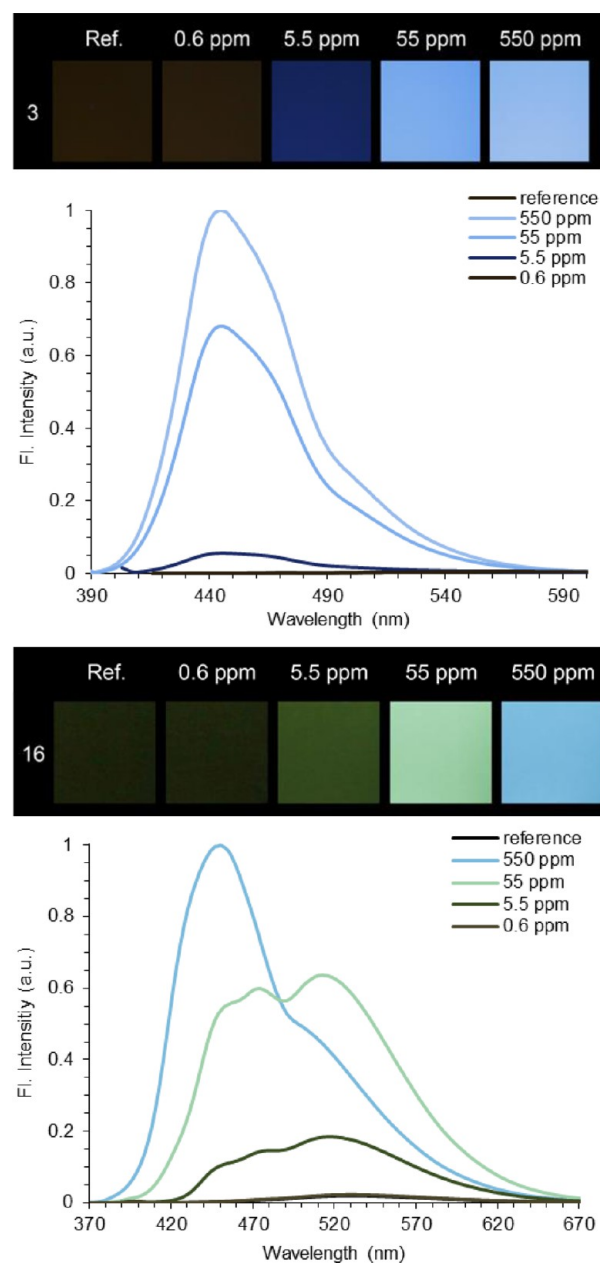


Figure 9. Photographs and fluorescence spectra of buffered aqueous solutions ($c = 4.4 \mu\text{M}$, pH 11) of **3** (top) and **16** (bottom) at the concentrations of 1,3-diaminopropane specified in the panel.

EXPERIMENTAL SECTION

All reagents and solvents were obtained from commercial suppliers and were used without further purification unless otherwise noted. Preparation of air- and moisture-sensitive materials was carried out in oven-dried flasks under a nitrogen atmosphere using Schlenk techniques. Compounds **5**,²² **10a**,²³ and **10b**¹⁵ were prepared as reported. ¹H NMR were recorded on a 300, 400, or 600 MHz spectrometer, and ¹³C NMR spectra were recorded on a 75, 100, or 150 MHz spectrometer. Chemical shifts (δ) are reported in parts per million (ppm) relative to traces of CHCl₃.²⁴ MS spectra were recorded using fast atom bombardment ionization, electrospray ionization, or matrix-assisted laser desorption/ionization methods detected by magnetic sector and FT-ICR techniques, respectively. Infrared (IR) spectra are reported in wavenumbers (cm⁻¹) and were recorded neat. Absorption spectra and emission spectra were recorded in dichloromethane and water/buffered solutions.

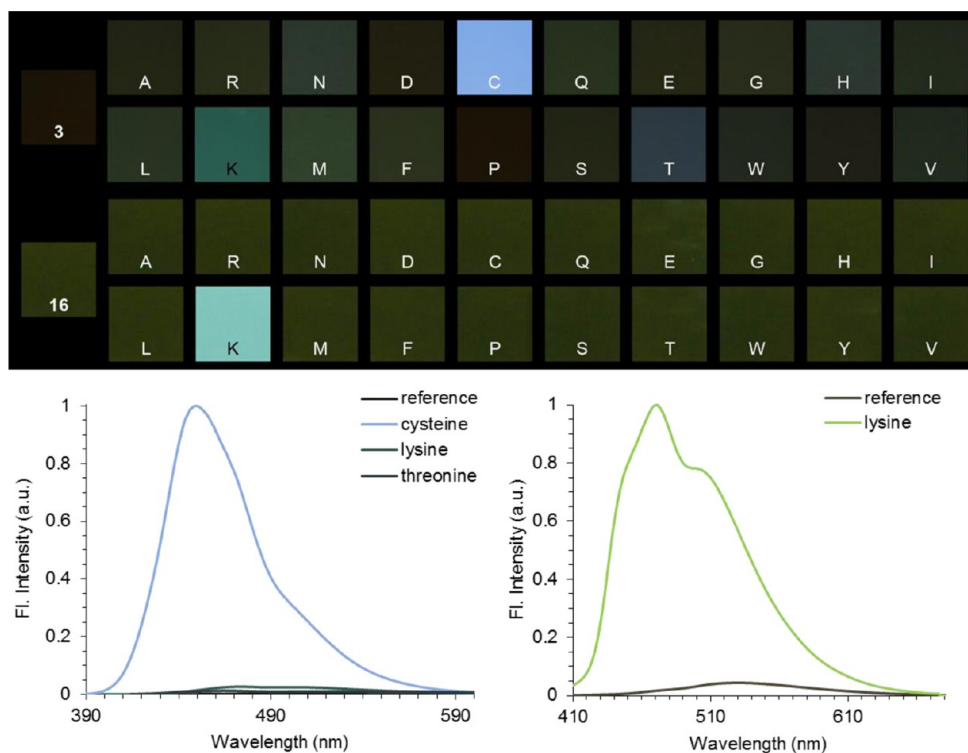


Figure 10. Photographs of buffered aqueous solutions ($c = 4.4 \mu\text{M}$, pH 11) of **3** and **16** after addition of amino acids (top) and fluorescence spectra of the respective solutions of **3** (bottom left) and **16** (bottom right). Photographs and spectra were obtained after 1 h. After 2 days the thioacetal of **16** had also fully formed.

13,13'-[(2,5-Diiodobenzene-1,4-diyl)bis(oxy)]bis-(2,5,8,11,15,18,21,24-octaoxapentacosane) (2). To a degassed solution of swallowtail tosylate (10.0 g, 18.6 mmol) in 2-butanone (50 mL) were added K_2CO_3 (7.00 g, 50.6 mmol) and diiodohydroquinone (3.05 g, 8.44 mmol). The mixture was stirred at 80°C for 4 days. The salts were filtered off through Celite with dichloromethane as eluent, and the filtrate was dried over MgSO_4 . The solvents were removed by rotary evaporation, and the crude product was purified by column chromatography (silica gel, petroleum ether/DCM/EtOAc/MeOH 5/3/1/0.6; $R_f = 0.18$) to give the desired product as a slightly yellow oil (7.81 g, 7.13 mmol, 85% yield). IR (cm^{-1}): 2868, 1462, 1348, 1299, 1249, 1200, 1099, 1051, 938, 849, 776, 540. ^1H NMR (300 MHz, CDCl_3): δ 7.44 (s, 2H), 4.38 (quin, $J = 5.0$ Hz, 2H), 3.77–3.60 (m, 48H), 3.56–3.52 (m, 8H), 3.37 (s, 12H). ^{13}C NMR (75 MHz, CDCl_3): δ 153.45, 126.12, 88.05, 80.95, 72.07, 71.33, 70.96–70.66, 59.18. HRMS (ESI): m/z $[\text{M} + \text{Na}]^+$ calcd for $\text{C}_{40}\text{H}_{72}\text{O}_{18}\text{I}_2\text{Na}$ 1117.2706, found 1117.2682.

4,4'-((1E,1'E)-(2,5-Bis(2,5,8,11,15,18,21,24-octaoxapentacosan-13-yloxy)-1,4-phenylene)bis(ethene-2,1-diyl))dibenzaldehyde (3). The reaction was performed in a heat-gun-dried 50 mL round-bottomed flask equipped with a condenser. Under a nitrogen atmosphere compound **2** (7.39 g, 6.75 mmol) and 4-ethenylbenzaldehyde (2.05 g, 15.5 mmol) were dissolved in dry DMF (150 mL). $\text{Pd}(\text{OAc})_2$ (60.6 mg, 270 μmol), tris(*o*-tolyl)phosphine (411 mg, 1.35 mmol), and triethylamine (7.5 mL) were added. The mixture was stirred at 100°C for 48 h. After the reaction mixture was cooled to ambient temperature, it was poured into 300 mL of water to give a yellow suspension, which was extracted with dichloromethane (5×100 mL). The combined organic layers were washed with brine and dried over MgSO_4 , and the solvents were removed under reduced pressure. The brown residue was purified by column chromatography (silica gel, petroleum ether/DCM/EtOAc/MeOH 5/3/1/0.6; $R_f = 0.14$) to give the desired compound as a viscous yellow oil (6.31 g, 5.72 mmol, 85% yield). IR (cm^{-1}): 2867, 1693, 1598, 1488, 1207, 1097, 964, 851, 809, 509. ^1H NMR (300 MHz, CDCl_3): δ 9.99 (s, 2H), 7.87 (d, $J = 8.3$ Hz, 4H), 7.69–7.64 (m, 6H), 7.38 (s, 2H), 7.15 (d, $J = 16.5$ Hz, 2H), 4.54 (quin, $J = 4.9$ Hz, 2H), 3.79–3.78 (m, 8H),

3.71–3.56 (m, 40H), 3.51–3.47 (m, 8H), 3.33 (s, 12H). ^{13}C NMR (75 MHz, CDCl_3): δ 191.7, 151.5, 144.1, 135.4, 130.4, 129.0, 128.1, 127.2, 126.9, 114.6, 79.9, 72.0, 71.2, 70.9–70.6, 59.1. HRMS (ESI): m/z $[\text{M} + \text{H}]^+$ calcd for $\text{C}_{58}\text{H}_{87}\text{O}_{20}$ 1103.5791, found 1103.5780; m/z $[\text{M} + \text{Na}]^+$ calcd for $\text{C}_{58}\text{H}_{86}\text{O}_{20}\text{Na}$ 1125.5610, found 1125.5593; m/z $[\text{M} + \text{K}]^+$ calcd for $\text{C}_{58}\text{H}_{86}\text{O}_{20}\text{K}$ 1141.5350, found 1141.5337. Anal. Calcd for $\text{C}_{58}\text{H}_{86}\text{O}_{20}$: C, 63.14; H, 7.86. Found: C, 62.77; H, 8.01.

13,13',13''-[(5-Bromobenzene-1,2,3-triyl)tris(oxy)]tris-(2,5,8,11,15,18,21,24-octaoxapentacosane) (6). Under a nitrogen atmosphere SwOTs (11.2 g, 20.9 mmol) was added to a suspension of potassium carbonate (6.57 g, 47.6 mmol) in 2-butanone (40 mL). After addition of 5-bromobenzene-1,2,3-triol (**5**; 1.30 g, 6.34 mmol) the reaction mixture was refluxed for 4 days. The reaction mixture was diluted with DCM and filtered over Celite. The solvent was removed under reduced pressure, and the crude product was purified by column chromatography (silica gel, petroleum ether/DCM/EtOAc/MeOH 5/3/1/1; $R_f = 0.20$) to give compound **6** as a yellow oil (8.27 g, 4.50 mmol, 71% yield). IR (cm^{-1}): 2867, 1582, 1471, 1455, 1350, 1300, 1246, 1223, 1096, 941, 849. ^1H NMR (300 MHz, CDCl_3): δ 6.85 (s, 2H), 4.43 (quin, $J = 5.1$ Hz, 2H), 4.31 (quin, $J = 5.0$ Hz, 1H), 3.69–3.50 (m, 84H), 3.36 (s, 18H). ^{13}C NMR (75 MHz, CDCl_3): δ 152.9, 138.5, 115.4, 113.7, 80.2, 78.4, 72.1, 71.1–70.5, 59.1. HRMS (ESI): m/z $[\text{M} + \text{K}]^+$ calcd for $\text{C}_{57}\text{H}_{107}^{81}\text{BrO}_{27}$ 1343.5800, found 1343.5794. Anal. Calcd for $\text{C}_{57}\text{H}_{107}\text{BrO}_{27}$: C, 52.49; H, 8.27; Br, 6.13. Found: C, 52.11; H, 8.23; Br, 6.31.

3,4,5-Tris(2,5,8,11,15,18,21,24-octaoxapentacosan-13-yloxy)benzaldehyde (7). To a solution of **6** (5.26 g, 4.04 mmol) in dry THF (200 mL) was added *n*-BuLi (9.00 mL of a 1.6 M solution in hexanes, 13.72 mmol) dropwise at -78°C , and the mixture was stirred for 1.5 h. Then *N*-formylpiperidine (1.25 mL, 11.3 mmol) was added slowly and the reaction mixture was stirred at -78°C for 4 h before it was quenched with a saturated aqueous NH_4Cl solution (50 mL) at 0°C . The layers were separated, and the aqueous layer was extracted with dichloromethane (5×50 mL). The combined organic layers were dried over MgSO_4 , and the solvents were evaporated. Purification by column chromatography (silica gel, petroleum ether/DCM/EtOAc/MeOH 5/3/1/1; $R_f = 0.24$) afforded the desired compound

as a pale yellow oil (3.57 g, 2.85 mmol, 71% yield). IR (cm^{-1}): 2867, 1692, 1581, 1442, 1350, 1327, 1298, 1246, 1199, 1093, 941, 849, 747. ^1H NMR (300 MHz, CDCl_3): δ 9.80 (s, 1H), 7.26 (s, 2H), 4.61–4.50 (m, 3H), 3.74–3.52 (m, 84H), 3.37 (s, 18H). ^{13}C NMR (75 MHz, CDCl_3): δ 191.3, 152.7, 144.8, 131.6, 111.1, 80.5, 78.1, 72.0, 71.1–70.6, 59.1. HRMS (ESI): m/z $[\text{M} + \text{Na}]^+$ calcd for $\text{C}_{58}\text{H}_{108}\text{O}_{28}\text{Na}$ 1275.6925, found 1275.6931; m/z $[\text{M} + \text{K}]^+$ calcd for $\text{C}_{58}\text{H}_{108}\text{O}_{28}\text{K}$ 1291.6664, found 1291.6629.

Trimethyl[3,4,5-tris(2,5,8,11,15,18,21,24-octaopentacosan-13-yloxy)phenyl]ethynylsilane (8). Under a nitrogen atmosphere **6** (4.87 g, 3.73 mmol) was dissolved in THF/TEA 1/1 (20 mL). The solution was thoroughly degassed, and TMS-acetylene (1.69 g, 17.2 mmol), triphenylphosphine (685 mg, 2.61 mmol), bis(triphenylphosphine)palladium(II) chloride (341 mg, 485 μmol), and copper iodide (334 mg, 1.75 mmol) were added. The reaction mixture was stirred at 65 $^\circ\text{C}$ for 20 h. After dilution with DCM the solvents were removed under reduced pressure. The residue was dissolved in DCM and the solvent evaporated twice. The crude product was purified by column chromatography (silica gel, petroleum ether/DCM/EtOAc/MeOH 5/3/1/1; R_f = 0.17) to give compound **8** as a yellow oil (4.51 g, 3.39 mmol, 91% yield). IR (cm^{-1}): 2868, 1568, 1455, 1350, 1247, 1097, 940, 843, 760. ^1H NMR (300 MHz, CDCl_3): δ 6.77 (s, 2H), 4.47 (quin, J = 5.0 Hz, 2H), 4.36 (quin, J = 4.9 Hz, 1H), 3.84–3.48 (m, 84H), 3.36 (s, 18H), 0.22 (s, 9H). ^{13}C NMR (75 MHz, CDCl_3): δ 151.9, 140.2, 117.8, 113.6, 105.2, 93.1, 80.3, 77.8, 72.1, 71.1–70.6, 70.5, 70.4, 59.1, 0.1. HRMS (ESI): m/z $[\text{M} + \text{Na}]^+$ calcd for $\text{C}_{62}\text{H}_{116}\text{O}_{27}\text{SiNa}$ 1343.7371, found 1343.7366. Anal. Calcd for $\text{C}_{62}\text{H}_{116}\text{O}_{27}\text{Si}$: C, 56.34; H, 8.85. Found: C, 56.07; H, 8.98.

13,13',13''-[5-Ethynylbenzene-1,2,3-triyl]tris(oxy)tris(2,5,8,11,15,18,21,24-octaopentacosane) (9). Under a nitrogen atmosphere **8** (4.35 g, 3.29 mmol) was dissolved in a degassed mixture of MeOH/THF 1/1 (40 mL). After addition of potassium fluoride dihydrate (1.55 g, 16.5 mmol) the reaction mixture was stirred at room temperature for 3 h. The solvent was evaporated under reduced pressure, and the crude product was purified by column chromatography (silica gel, petroleum ether/DCM/EtOAc/MeOH; R_f = 0.19) to give compound **9** as a pale yellow oil (3.92 g, 3.13 mmol, 95% yield). IR (cm^{-1}): 2868, 1570, 1454, 1420, 1350, 1328, 1230, 1240, 1199, 1094, 943, 849. ^1H NMR (400 MHz, CDCl_3): δ 6.82 (s, 2H), 4.45 (quin, J = 5.0 Hz, 2H), 4.37 (quin, J = 4.9 Hz, 1H), 3.72–3.50 (m, 84H), 3.36 (s, 18H), 2.97 (s, 1H). ^{13}C NMR (100 MHz, CDCl_3): δ 152.0, 140.5, 116.7, 114.1, 83.7, 80.3, 78.1, 76.4, 72.0, 71.1–70.6, 70.5, 59.1. HRMS (ESI): m/z $[\text{M} + \text{Na}]^+$ calcd for $\text{C}_{59}\text{H}_{108}\text{O}_{27}\text{Na}$ 1271.6976, found 1271.6970.

Diethyl 4-[(E)-2-[4-(Diethoxymethyl)phenyl]ethenyl]benzylphosphonate (11). The bisphosphonate **10a** (2.21 g, 5.84 mmol) was dissolved in dry THF (10 mL), and the solution was cooled to 0 $^\circ\text{C}$. KO^tBu (587 mg, 5.23 mmol) was added slowly, and the mixture was stirred 5 min before the aldehyde (930 μL , 4.67 mmol) was added as quickly as possible. The reaction mixture was stirred at 0 $^\circ\text{C}$ for 45 min. Then the reaction was quenched by adding a saturated aqueous NH_4Cl solution (8 mL). The layers were separated, and the aqueous layer was extracted with dichloromethane (4 \times 20 mL). The combined organic layers were dried over MgSO_4 and the solvents were evaporated. The bright yellow crude product was purified by column chromatography (silica gel, EtOAc + 2% diethylamine; R_f = 0.30) and a second column (EtOAc/petroleum ether + 2% diethylamine 2/1; R_f = 0.13) to give the desired product as a bright yellow oil (410 mg, 1.10 mmol, 21%). IR (cm^{-1}): 2974, 1515, 1247, 1095, 1047, 1020, 958, 849, 571, 528. ^1H NMR (600 MHz, CDCl_3): δ 7.49 (d, J = 8.4 Hz, 2H), 7.45 (d, J = 8.0 Hz, 4H), 7.28 (dd, J = 8.4 Hz, J = 2.3 Hz, 2H), 7.08 (s, 2H), 5.50 (s, 1H), 4.05–3.98 (m, 4H), 3.64–3.50 (m, 4H), 3.17 (s, 1H), 3.13 (s, 1H), 1.26–1.22 (m, 12H). ^{13}C NMR (150 MHz, CDCl_3): δ 138.5, 137.4, 136.0 (d, J = 4.0 Hz), 131.1 (d, J = 9.8 Hz), 130.2 (d, J = 6.7 Hz), 128.5 (d, J = 2.3 Hz), 128.3 (d, J = 1.8 Hz), 127.1, 126.7 (d, J = 3.3 Hz), 101.4, 62.2 (d, J = 6.7 Hz), 61.1, 34.1, 33.2, 16.5 (d, J = 6.0 Hz), 15.3. ^{31}P NMR (121 MHz, CDCl_3): δ 26.15. HRMS (ESI): m/z $[\text{M} + \text{H}]^+$ calcd for $\text{C}_{24}\text{H}_{34}\text{O}_5\text{P}$ 433.2144, found 433.2136. Anal. Calcd for $\text{C}_{24}\text{H}_{34}\text{O}_5\text{P}$: C, 66.65; H, 7.69; P, 7.16. Found: C, 66.66; H, 7.56; P, 7.35.

13,13',13''-[5-[(E)-2-(4-[(E)-2-[4-(Diethoxymethyl)phenyl]ethenyl]phenyl)ethenyl]benzene-1,2,3-triyl]tris(oxy)tris(2,5,8,11,15,18,21,24-octaopentacosane) (12). To a solution of **11** (278 mg, 0.64 mmol) in dry THF (15 mL) was added KO^tBu (114 mg, 1.02 mmol) at 0 $^\circ\text{C}$. The suspension was stirred at 0 $^\circ\text{C}$ for 15 min, and then 4-(diethoxymethyl)benzaldehyde (1.02 g, 813 μmol) was added dropwise. The reaction mixture was stirred at 0 $^\circ\text{C}$ for an additional 20 min before it was warmed to room temperature and stirred for 24 h. The reaction was quenched with 10 mL of a saturated aqueous NH_4Cl solution. The layers were separated, and the aqueous layer was extracted with dichloromethane (5 \times 30 mL). The combined organic layers were dried over MgSO_4 , and the solvents were removed under reduced pressure. The product was used in the next step without further purification.

4-[(E)-2-(4-[(E)-2-[3,4,5-Tris(2,5,8,11,15,18,21,24-octaopentacosan-13-yloxy)phenyl]ethenyl]phenyl)ethenyl]benzaldehyde (13). **12** was dissolved in toluene (50 mL), and a catalytic amount of iodine was added. The solution was refluxed for 5 h and then quenched with 10 mL of a saturated aqueous sodium bisulfite solution. The layers were separated, and the aqueous layer was extracted with dichloromethane (5 \times 30 mL). The combined organic layers were dried over MgSO_4 , and the solvents were evaporated. Purification by column chromatography (silica gel, petroleum ether/DCM/EtOAc/MeOH 5/3/1/1; R_f = 0.22) afforded the desired compound as a bright yellow oil (403 mg, 276 μmol , 41% yield over two steps). IR (cm^{-1}): 2868, 1693, 1594, 1453, 1434, 1349, 1305, 1249, 1199, 1093, 964, 845, 793, 538. ^1H NMR (300 MHz, CDCl_3): δ 9.98 (s, 1H), 7.86 (d, J = 8.2 Hz, 2H), 7.65 (d, J = 8.2 Hz, 2H), 7.54–7.48 (m, 4H), 7.25 (d, J = 16.4 Hz, 1H), 7.14 (d, J = 16.4 Hz, 1H), 7.01 (d, J = 16.4 Hz, 1H), 6.94 (d, J = 16.4 Hz, 1H), 6.87 (s, 2H), 4.56 (quin, J = 5.0 Hz, 2H), 4.38 (quin, J = 4.8 Hz, 1H), 3.77–3.49 (m, 84H), 3.35 (s, 6H), 3.34 (s, 12H). ^{13}C NMR (75 MHz, CDCl_3): δ 191.6, 152.3, 143.6, 139.2, 137.7, 135.8, 135.4, 132.6, 131.9, 130.3, 129.1, 127.5, 127.4, 127.1, 126.0, 108.6, 80.3, 77.9, 72.0, 71.0, 71.0–70.4, 59.1. HRMS (ESI): m/z $[\text{M} + \text{H}]^+$ calcd for $\text{C}_{74}\text{H}_{121}\text{O}_{28}$ 1457.8044, found 1457.8092; m/z $[\text{M} + \text{Na}]^+$ calcd for $\text{C}_{74}\text{H}_{120}\text{O}_{28}\text{Na}$ 1479.7864, found 1479.7867; m/z $[\text{M} + \text{K}]^+$ calcd for $\text{C}_{74}\text{H}_{120}\text{O}_{28}\text{K}$ 1495.7603, found 1495.7617.

1,4-Bis[(E)-2-[4-(diethoxymethyl)phenyl]ethenyl]-2,5-diiodobenzene (14). Under a nitrogen atmosphere tetraethyl ((2,5-diiodo-1,4-phenylene)bis(methylene))bis(phosphonate) (**10b**; 4.00 g, 6.35 mmol) was dissolved in dry THF (50 mL) and cooled to 0 $^\circ\text{C}$. Potassium *tert*-butoxide (1.50 g, 13.3 mmol) was added, and the reaction mixture was stirred for 10 min before warming it to room temperature. After addition of 4-(diethoxymethyl)benzaldehyde (2.78 g, 13.3 mmol) the reaction was stirred for 1 h at room temperature and quenched with MeOH (100 mL), resulting in precipitation of a yellow solid. The mixture was cooled in the freezer overnight. The precipitate was filtered off and washed with an excess of MeOH to give compound **14** (3.42 g, 4.64 mmol, 73% yield) as a yellow solid. Mp: 177 $^\circ\text{C}$. IR (cm^{-1}): 2971, 2926, 2876, 1509, 1454, 1329, 1211, 1114, 1094, 1061, 945, 850, 791, 692, 497. ^1H NMR (300 MHz, CDCl_3): δ 8.08 (s, 2H), 7.55 (d, J = 8.4 Hz, 4H), 7.50 (d, J = 8.3 Hz, 4H), 7.20 (d, J = 16.0 Hz, 2H), 6.98 (d, J = 16.0 Hz, 2H), 5.53 (s, 2H), 3.70–3.47 (m, 8H), 1.26 (t, J = 7.1 Hz, 12H). ^{13}C NMR (75 MHz, CDCl_3): δ 140.9, 139.5, 136.7, 136.5, 132.2, 130.8, 127.3, 126.9, 101.4, 100.4, 61.2, 15.4. HRMS (FAB): m/z $[\text{M}]^+$ calcd for $\text{C}_{32}\text{H}_{36}\text{I}_2\text{O}_4$ 738.0703, found 738.0699.

13,13',13'',13''',13''''-[2,5-Bis[(E)-2-[4-(diethoxymethyl)phenyl]ethenyl]benzene-1,4-diyl]bis[ethyne-2,1-diyl]benzene-5,1,2,3-tetrayltris(oxy)]hexakis(2,5,8,11,15,18,21,24-octaopentacosane) (15). Under a nitrogen atmosphere **9** (1.34 g, 1.07 mmol) was dissolved in a mixture of toluene/piperidine 2/1 (12 mL). The solution was thoroughly degassed, and **14** (330 mg, 447 μmol), bis(triphenylphosphine)palladium(II) chloride (15.7 mg, 22.3 μmol), and copper iodide (4.26 mg, 22.3 μmol) were added. The reaction mixture was stirred at 45 $^\circ\text{C}$ for 16 h. After dilution with DCM the solvents were removed under reduced pressure. The residue was redissolved in DCM and the solvent removed under reduced pressure twice. The crude product was purified by column chromatography (silica gel, EtOAc/MeOH 7/3; R_f = 0.18) to give

compound **15** (1.23 g, 413 μmol , 93% yield) as a yellowish oil. IR (cm^{-1}): 2869, 1568, 1494, 1454, 1349, 1241, 1095, 849, 729. ^1H NMR (400 MHz, CDCl_3): δ 7.89 (s, 2H), 7.61 (d, $J = 16.3$ Hz, 2H), 7.56 (d, $J = 8.1$ Hz, 4H), 7.47 (d, $J = 8.0$ Hz, 4H), 7.28 (d, $J = 16.3$ Hz, 2H), 6.93 (s, 4H), 5.50 (s, 2H), 4.54 (quin, $J = 4.7$ Hz, 4H), 4.42 (quin, $J = 4.9$ Hz, 2H), 3.77–3.47 (m, 176H), 3.34 (s, 12H), 3.32 (s, 24H), 1.23 (t, $J = 7.0$ Hz, 12H). ^{13}C NMR (100 MHz, CDCl_3): δ 152.1, 140.3, 139.1, 137.4, 137.2, 130.7, 129.1, 127.3, 126.8, 125.7, 122.4, 117.7, 113.3, 101.3, 95.8, 86.9, 80.4, 78.0, 72.0, 72.0, 71.0–70.4, 61.0, 59.1, 59.1, 15.4. HRMS (MALDI): m/z $[\text{M}]^+$ calcd for $\text{C}_{150}\text{H}_{251}\text{O}_{58}$ 2980.6686, found 2980.6785.

4,4'-(2,5-Bis[[3,4,5-tris(2,5,8,11,15,18,21,24-octaoxapentacosan-13-yloxy)phenyl]ethynyl]benzene-1,4-diyl)di-(E)-ethene-2,1-diyl]dibenzaldehyde (16). **15** (500 mg, 168 μmol) was dissolved in a mixture of THF/water 3/1 (33 mL). A catalytic amount of trifluoroacetic acid was added, and the reaction mixture was stirred at room temperature for 16 h. After quenching with a saturated aqueous solution of sodium bicarbonate (3 mL) and extraction with DCM (2 \times 50 mL, 3 \times 20 mL) the combined organic layers were dried over MgSO_4 . The solvent was evaporated under reduced pressure and the crude product purified by column chromatography (silica gel, petroleum ether/DCM/EtOAc/MeOH 5/3/1/1.5; $R_f = 0.42$), to give compound **16** (444 mg, 157 μmol , 93% yield) as a yellowish oil. IR (cm^{-1}): 2868, 1694, 1599, 1567, 1494, 1454, 1349, 1240, 1096, 942, 849, 528. ^1H NMR (300 MHz, CDCl_3): δ 10.00 (s, 2H), 7.96–7.88 (m, 6H), 7.82–7.71 (m, 6H), 7.36 (d, $J = 16.3$ Hz, 2H), 6.94 (s, 4H), 4.54 (quin, $J = 4.9$ Hz, 4H), 4.42 (quin, $J = 4.76$ Hz, 2H), 3.78–3.46 (m, 168H), 3.35 (s, 12H), 3.32 (s, 24H). ^{13}C NMR (75 MHz, CDCl_3): δ 191.7, 152.2, 143.2, 140.5, 137.3, 135.8, 130.5, 130.0, 129.4, 128.9, 127.4, 122.9, 117.4, 113.3, 96.5, 86.47, 80.5, 78.0, 72.0, 72.0, 71.0–70.4, 59.1, 59.1. HRMS (MALDI): m/z $[\text{M}]^+$ calcd for $\text{C}_{142}\text{H}_{231}\text{O}_{56}$ 2832.5223, found 2832.5181. Anal. Calcd for $\text{C}_{142}\text{H}_{231}\text{O}_{56}$: C, 60.20; H, 8.18. Found: C, 59.72; H, 8.18.

■ ASSOCIATED CONTENT

● Supporting Information

Figures giving ^1H and ^{13}C NMR spectra of **6–9**, **11**, and **13–16** as well as tables giving the Cartesian coordinates of computational data for **16m**. This material is available free of charge via the Internet at <http://pubs.acs.org>.

■ AUTHOR INFORMATION

Corresponding Author

*E-mail: uwe.bunz@oci.uni-heidelberg.de; dreuw@uni-heidelberg.de.

Notes

The authors declare no competing financial interest.

■ REFERENCES

- Phillips, R. L.; Kim, I. B.; Tolbert, L. M.; Bunz, U. H. F. *J. Am. Chem. Soc.* **2008**, *130*, 6952–6955.
- (a) Merchant, Z. M.; Cheng, S. G. G. In *Characterization of Foods, Emerging Methods*; Gaonkar, A. G., Ed.; Elsevier Science: New York, 1995; Chapter 15. (b) Bao, B.; Yuwen, L.; Zheng, X.; Weng, L.; Zhu, X.; Zhan, X.; Wang, L. *J. Mater. Chem.* **2010**, *20*, 9628–9634. (c) Ajayakumar, M. R.; Mukhopadhyay, P. *Chem. Commun.* **2009**, 3702–3704. (d) Kçrsten, S.; Mohr, G. J. *Chem. Eur. J.* **2011**, *17*, 969–975. (e) Mohr, G. J. *Chem. Eur. J.* **2004**, *10*, 1082–1090. (f) Mohr, G. J.; Demuth, C.; Spichinger-Keller, U. E. *Anal. Chem.* **1998**, *70*, 3868–3873.
- (a) Rakow, N. A.; Sen, A.; Janzen, M. C.; Ponder, J. B.; Suslick, K. S. *Angew. Chem.* **2005**, *117*, 4604–4608; (b) *Angew. Chem., Int. Ed.* **2005**, *44*, 4528–4532.
- (a) Greene, N. T.; Shimizu, K. D. *J. Am. Chem. Soc.* **2005**, *127*, 5695–5700. (b) Merchant, Z. M.; Cheng, S. G. G. In *Characterization of Foods, Emerging Methods*; Gaonkar, A. G., Ed.; Elsevier Science: New York, 1995; Chapter 15. (c) Zhou, H. C.; Baldini, L.; Hong, J.; Wilson, A. J.; Hamilton, A. D. *J. Am. Chem. Soc.* **2006**, *128*, 2421–2425.
- (d) Yeh, C. Y.; Lin, S. J.; Hwang, D. F. *J. Food Drug Anal.* **2004**, *12*, 128–132.
- (a) Wiskur, S. L.; Ait-Haddou, H.; Lavigne, J. J.; Anslyn, E. V. *Acc. Chem. Res.* **2001**, *34*, 963–972. (b) Lavigne, J. J.; Anslyn, E. V. *Angew. Chem., Int. Ed.* **1999**, *38*, 3666–3669.
- Bao, B.; Yuwen, L.; Zheng, X.; Weng, L.; Zhu, X.; Zhan, X.; Wang, L. *J. Mater. Chem.* **2010**, *20*, 9628–9634.
- (a) Ajayakumar, M. R.; Mukhopadhyay, P. *Chem. Commun.* **2009**, 3702–3704. (b) Kçrsten, S.; Mohr, G. J. *Chem. Eur. J.* **2011**, *17*, 969–975. (c) Mohr, G. J. *Chem. Eur. J.* **2004**, *10*, 1082–1090. (d) Mohr, G. J.; Demuth, C.; Spichinger-Keller, U. E. *Anal. Chem.* **1998**, *70*, 3868–3873.
- (a) Nelson, T. L.; O'Sullivan, C.; Greene, N. T.; Maynor, M. S.; Lavigne, J. J. *J. Am. Chem. Soc.* **2006**, *128*, 5640–5641. (b) Maynor, M. S.; Nelson, T. L.; O'Sullivan, C.; Lavigne, J. J. *Org. Lett.* **2007**, *9*, 3217–3220. (c) Nelson, T. L.; Tran, I.; Ingallina, T. G.; Maynor, M. S.; Lavigne, J. J. *Analyst* **2007**, *132*, 1024–1030.
- (a) Mertz, E.; Zimmerman, S. C. *J. Am. Chem. Soc.* **2003**, *125*, 3424–3425. (b) Mertz, E.; Beil, J. B.; Zimmerman, S. C. *Org. Lett.* **2003**, *5*, 3127–3130.
- (a) Feustler, E. K.; Glass, T. E. *J. Am. Chem. Soc.* **2003**, *125*, 16174–16175. (b) Secor, K.; Plante, J.; Avetta, C.; Glass, T. E. *J. Mater. Chem.* **2005**, *15*, 4073–4077.
- Kumpf, J.; Bunz, U. H. F. *Chem. Eur. J.* **2012**, *18*, 8921–8924.
- (a) Zuccherro, A. J.; McGrier, P. L.; Bunz, U. H. F. *Acc. Chem. Res.* **2010**, *43*, 397–408. (b) Hauck, M.; Schönhaber, J.; Zuccherro, A. J.; Hardcastle, K. I.; Müller, T. J. J.; Bunz, U. H. F. *J. Org. Chem.* **2007**, *72*, 6714–6725. (c) Zuccherro, A. J.; Wilson, J. N.; Bunz, U. H. F. *J. Am. Chem. Soc.* **2006**, *128*, 11872–11881. (d) Davey, E. A.; Zuccherro, A.; Trapp, O.; Bunz, U. H. F. *J. Am. Chem. Soc.* **2011**, *133*, 7716–7718. (e) Schwaebel, T.; Trapp, O.; Bunz, U. H. F. *Chem. Sci.* **2013**, *4*, 273–281. (f) Gerhardt, W. W.; Zuccherro, A. J.; Wilson, J. N.; South, C. R.; Bunz, U. H. F.; Weck, M. *Chem. Commun.* **2006**, 2141–2143. (g) Tolosa, J.; Solntsev, K. M.; Tolbert, L. M.; Bunz, U. H. F. *J. Org. Chem.* **2010**, *75*, 523–534. (h) Tolosa, J.; Zuccherro, A. J.; Bunz, U. H. F. *J. Am. Chem. Soc.* **2008**, *130*, 6498–6506.
- (a) McGrier, P. L.; Solntsev, K. M.; Miao, S.; Tolbert, L. M.; Miranda, O. R.; Rotello, V. M.; Bunz, U. H. F. *Chem. Eur. J.* **2008**, *14*, 4503–4510. (b) Patze, C.; Broedner, K.; Rominger, F.; Trapp, O.; Bunz, U. H. F. *Chem. Eur. J.* **2011**, *17*, 13720–13725.
- Schwaebel, T.; Schäfer, V.; Wenz, J.; Coombs, B. A.; Tolosa, J.; Bunz, U. H. F. *J. Org. Chem.* **2013**, *78*, 960–965.
- Wilson, J. N.; Windscheif, P. M.; Evans, U.; Myrick, M. L.; Bunz, U. H. F. *Macromolecules* **2002**, *35*, 8681–8683.
- (a) Casida, M. E. In *Recent Advances in Density Functional Theory*; Chong, D. P., Ed.; World Scientific: Singapore, 1995; Part I, pp 145–192. (b) Dreuw, A.; Head-Gordon, M. *Chem. Rev.* **2005**, *105*, 4009–4037.
- Neese, F. *WIREs Comput. Mol. Sci.* **2012**, *2*, 73–78.
- Schäfer, A.; Klamt, A.; Sattel, D.; Lohrenz, J. C. W.; Eckert, F. *Phys. Chem. Chem. Phys.* **2000**, *2*, 2187–2192.
- Plötner, J.; Tozer, D. J.; Dreuw, A. *J. Chem. Theo. Comp.* **2010**, *6*, 2315–2324.
- Head-Gordon, M.; Grana, A. M.; Maurice, D.; White, C. A. *J. Phys. Chem.* **1995**, *99*, 14261–14268.
- (a) Sprung, M. M. *Chem. Rev.* **1940**, *26*, 297–336. (b) Layer, R. W. *Chem. Rev.* **1963**, *63*, 489–510. (c) Dayagi, S. In *The chemistry of the carbon-nitrogen double bond*; Patai, S., Ed.; Wiley: New York, 1970; pp 61–147.
- Yasuda, T.; Shimizu, T.; Liu, F.; Ungar, G.; Kato, T. *J. Am. Chem. Soc.* **2011**, *133*, 13437–13444.
- Winter, A.; Friebe, C.; Hager, M. D.; Schubert, U. S. *Eur. J. Org. Chem.* **2009**, 801–809.
- Fulmer, G. R.; Miller, A. J. M.; Sherden, N. H.; Gottlieb, H. E.; Nudelman, A.; Stoltz, B. M.; Bercaw, J. E.; Goldberg, K. I. *Organometallics* **2010**, *29*, 2176–2179.